◎ 논 문

Optimization of Rotor Blade Stacking Line Using Three Different Surrogate Models

Choon-Man Jang*, Abdus Samad**, Kwang-Yong Kim**

Key Words : Optimization, Axial Compressor, Surrogate Models, Blade Sweep, Blade Lean, Blade Skew, Adiabatic Efficiency

ABSTRACT

This paper describes the shape optimization of rotor blade in a transonic axial compressor rotor. Three surrogate models, Kriging, radial basis neural network and response surface methods, are introduced to find optimum blade shape and to compare the characteristics of object function at each optimal design condition. Blade sweep, lean and skew are considered as design variables and adiabatic efficiency is selected as an objective function. Throughout the shape optimization of the compressor rotor, the predicted adiabatic efficiency has almost same value for three surrogate models. Among the three design variables, a blade sweep is the most sensitive on the object function. It is noted that the blade swept to backward and skewed to the blade pressure side is more effective to increase the adiabatic efficiency in the axial compressor. Flow characteristics of an optimum blade are also compared with the results of reference blade.

1. Introduction

Study on the optimum design of a rotor blade in a transonic axial compressor is important to enhance rotor performance.

In the blade shape optimization of an axial compressor rotor, the use of blade lean (dihedral), sweep, and skew (stacking line in rotational direction) has become a matter of interest in the design of turbomachinery blades. These shape parameters which form a three-dimensional stacking line is introduced to reduce shock losses, corner separation in the blade hub, and tip clearance losses in a transonic compressor rotor.

One of the most significant design trends in a transonic compressor rotor is the use of aerodynamic sweep. Watanabe and Zangeneh[1] reported that the blade sweep in the design of a transonic turbomachinery blade is an effective parameter to control the strength and position of the shock wave at the tip of the transonic rotors. Denton and Xu[2] investigated the effects of sweep and lean on the performance of a transonic fan and showed that the stall margin was significantly improved with the forward swept blade although a very little change in the peak efficiency was produced by the blade sweep or lean.

There are a number of studies on the advantages of a skewed rotor. Fischer, et al.[3] reported the effect of bowed stators on the performance of a compressor,

* Fire & Eng. Services R. D., Korea Institute of Construction Technology
E-mail : jangcm@kict.re.kr
** Department of Mechanical Eng., Inha University

Table 1 Design specifications of NASA rotor 37

Mass flow, kg/s	20.19
Rotational speed, rpm	17188.7
Pressure ratio	2.106
Inlet hub-tip ratio	0.7
Inlet tip relative Mach no.	1.4
Inlet hub relative Mach no.	1.13
Tip solidity	1.288
Rotor aspect ratio	1.19
Number of rotor blades	36

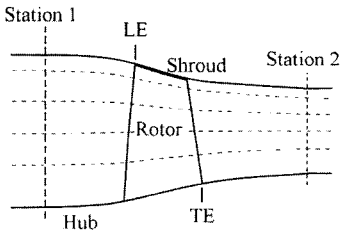

Fig. 1 Meridional view of Rotor 37

and showed that the separation was reduced in the bowed stator leading to increase in the stagnation pressure ratio and efficiency.

The authors investigated to understand the effects of design parameters on the performance of an axial compressor rotor and stator[4),(5)]. Jang et al.[5] has shown by shape optimization of an axial compressor blade using blade sweep, lean and skew as variables that efficiency is enhanced by suppressing the separation area on the blade suction surface.

On the other hand, surrogate models are being used widely in multidisciplinary optimization. Queipo et al.[6] reviewed various surrogate based models used in aerospace applications. Shyy et al.[7] applied global optimization methods to design rocket engine. Samad et al.[8] applied multiple surrogate models on the optimization of an axial compressor rotor using the design variables of blade sweep, lean and skew. They reported that the weighted averaged multiple surrogate models show good overall performance to predict the optimum values of the objective functions.

In the present study, three surrogate models combining with three-dimensional Navier-Stokes solver are introduced to find optimum blade shape of a transonic axial compressor operating at the design flow condition. That is, Kriging, radial basis neural network and response surface methods are compared to evaluate their effects on object function, and blade sweep, lean and skew are considered as design variables. The effect of each variable on performance is also analyzed. Detailed internal flow analysis is performed in relation with the efficiency enhancement.

2. Test Axial Compressor

NASA rotor 37[9], which is a low-aspect ratio axial-flow compressor rotor, is considered in the present shape optimization problem. The detailed specifications of the compressor are summarized in Table 1. The rotor tip clearance is 0.356 mm (0.45 percent span). The measured choking mass flow rate is 20.93 kg/s, which corresponds to 103.67% of the design flow rate[9].

The meridional view of the axial compressor is shown in Fig. 1. Total pressure, total temperature, and adiabatic efficiency in relation with the mass flow rates are measured at inlet (station 1) and outlet (station 2) positions as shown in Fig. 1. The inlet and outlet positions are located at 41.9 mm upstream of the tip leading edge of the rotor and at 101.9 mm downstream of the tip trailing edge of the rotor, respectively.

3. Shape Optimization of Rotor Blade

3.1. Surrogate Models

Three different surrogate models, Kriging (KRG), radial basis neural network (RBNN) and response surface (RSM) methods are introduced to optimize the shape of rotor blade and to compare their results on compressor rotor performance.

To optimize the blade shape, initially an objective function is defined. Design variables are selected among the variables for which objective function is

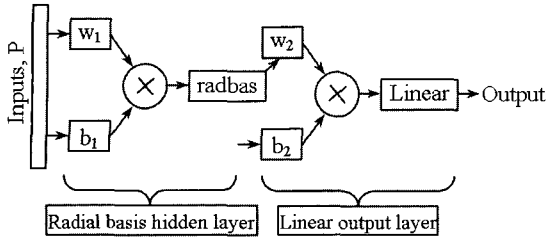

Fig. 2 Radial basis network (single neuron)

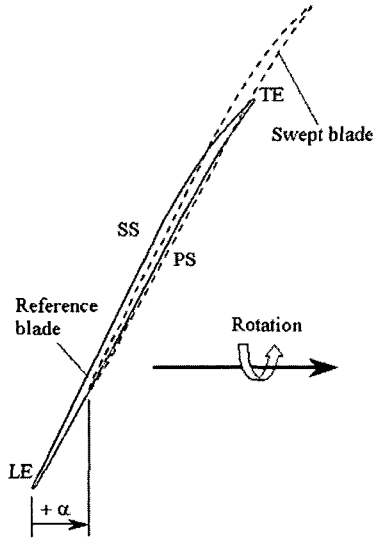

Fig. 3 Definition of blade sweep(top view)

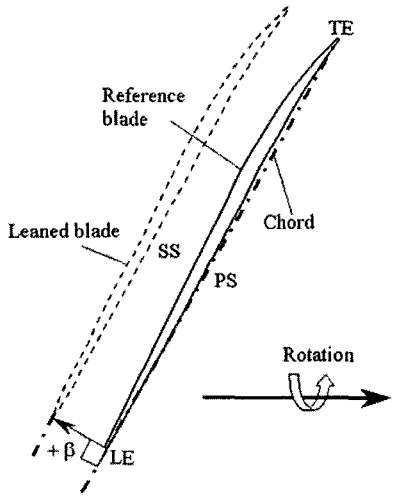

Fig. 4 Definition of blade lean (top view)

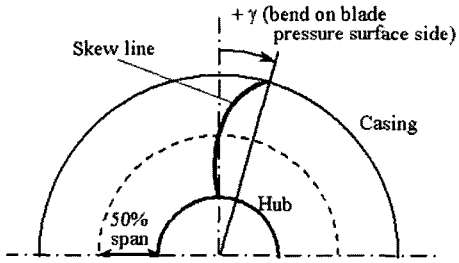

Fig. 5 Definition of blade skew (front view)

sensitive, In the next step, the value of objective function at each experimental point is obtained by numerical analysis. Finally, surrogates are constructed to obtain the optimal points.

For the curve fitting of experimental points, Kriging method adopts deterministic technique where RSM is simply a regression analysis to fit a second order approximate curve.

RSM[10], which is a global optimization method, does not require calculation of the local sensitivity of each design variable, and is able to perform tasks in parallel easily. The RSM can utilize information collected from various sources and by different tools. Thus, this method is effective for both of single- and multi-disciplinary optimization problems.

In order to reduce the number of data needed for constructing a response surface, the design of experiment (DOE) is important for selecting design points. D-optimal design[11] is employed in the present work for sampling points in design space. Design space is constituted by the upper and lower limits of the variables.

Kriging method (KRG)[12] uses spatial correlation information and estimates the analysis results in the sampling points. Linear polynomial function with Gauss correlation function is used for model construction in KRG. Kriging postulation is the combination of global model and local departures of the following form:

$$\hat{F}(x) = f(x) + Z(x) \quad (1)$$

where $\hat{F}(x)$ represents the unknown function, f(x)

is the known function of x, and Z(x) is the realization of a stochastic process with mean zero and non-zero covariance. A linear function, f(x) is fitted first, and real points are interpolated on it to get mean zero. Here, f(x) is global design space, while Z(x) is the localized deviations.

Radial basis neural network method (RBNN)[13] is a two layer network and uses a radial basis transfer function in its hidden layer and a linear function in its output layer as shown in Fig. 2. The design parameters for this function are spread constant (SC) and a user defined error goal (EG). SC value is selected in such a way that should not be so large that each neuron will respond same for the all input, and that should not be so small that the network will be very high sensitive for every input within design space. EG or mean square error goal selection is also important. A very small error goal will produce over training of the network while a large error goal will influence the accuracy of the model. Allowable error goal is decided from the allowable error from the mean input responses. In MATLAB[14], *newrb* is the function for RBNN design.

3.2. Objective Function and Design Variables

In the present study, adiabatic efficiency is selected as an objective function of the optimization.

To enhance the adiabatic efficiency of the compressor rotor, three-dimensional blade stacking line is optimized by introducing three shape variables; namely sweep, lean, and skew as shown in Figs. 3-5. The term of sweep is used to describe movement of airfoil section in the manner shown in Fig. 3. That is, movement parallel to the airfoil chord line is termed sweep. A sweep value, α in Fig. 3, is defined at the rotor tip and normalized by the axial tip chord (= 27.77 mm). The blade sweep is taken to be positive if the airfoil sections are moved in the downstream direction. The line of the swept blade between the rotor tip (α in Fig. 3) and hub (= zero) is linearly connected while the gap of the tip clearance is kept constant.

Table 2 Design space of blade sweep, lean, and skew

Variables		Lower Bound	Middle	Upper Bound
Sweep (a)	%	0.0	12.6	25.2
Lean (b)	%	-3.6	-1.8	0.0
Skew (g)	rad.	0.0	0.05	0.1

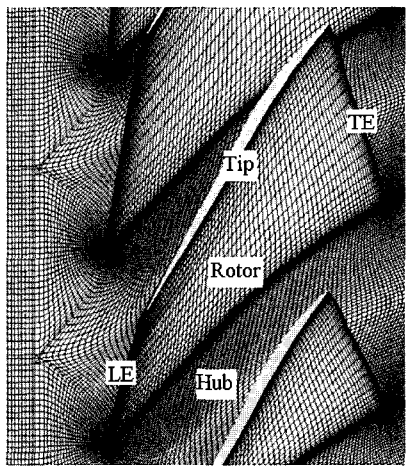

Fig. 6 Computational grids

Figure 4, which is top view of the rotor, shows the definition of blade lean (or dihedral). Lean is defined when the blade moves normal to the airfoil chord line. The lean value, β in Fig. 4, is defined at the rotor tip and normalized by the axial tip chord. The blade lean is taken to be positive if the airfoil sections are moved to the blade suction side. The value of blade lean is zero at hub, and is linearly connected to the rotor tip keeping constant tip clearance.

Finally, a skew line is introduced to optimize the blade stacking as shown in Fig. 5. The skew angle defined at rotor tip, γ in Fig. 5, is taken to be positive if the skew line of the rotor tip bends to the blade pressure surface side. The skew line is formed by a second order polynomial curve. To complete the skew line, skew angles at hub and at 50 percent span are set to zeros.

The range of each variable for selection of the points for response evaluation is determined by preliminary calculations, and is summarized in Table 2.

Table 3 Optimum value of design variables

Design Variables	KRG	RBNN	RSM
Sweep (a) %	11.7	10.4	10.2
Lean (b) %	-0.1	0.0	-0.9
Skew (g) rad.	0.064	0.061	0.059

Table 4 Predicted and calculated values of adiabatic efficiency at optimal condition

Models	Ref. %	Predicted Eff. % (Fp)	Calculated Eff. % (Fc)	Error % (Fp-Fc)/Fp	Increase to Ref. %
KRG	88.65	90.10	89.82	0.3107	1.31
RBNN		90.06	89.92	0.1555	1.43
RSM		90.07	89.85	0.2443	1.35

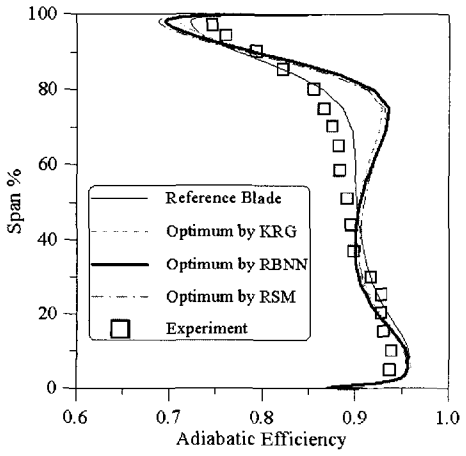

Fig. 7 Spanwise distribution of efficiency

3.3. Numerical Analysis Method

The three-dimensional thin-layer Navier-Stokes and energy equations are solved on body-fitted grids using an explicit finite-difference scheme. An explicit Runge-Kutta scheme proposed by Jameson, et al.[15] is used to solve flow from initial to steady state with a spatially varying time step to accelerate convergence. Artificial dissipation terms have been added to resolve shocks. The algebraic turbulence model of Baldwin and Lomax[16] has been employed to estimate the eddy viscosity.

A composite grid system with structured H-,C-, and O-type grids is adopted to represent the complicated configuration of the axial compressor.

Figure 6 shows the computational grids. H-type grid consists of 60X36X63 grids (in the streamwise, pitchwise and spanwise directions, respectively), and is introduced for the inlet flow region. C-type grid consists of 350X46X63 grids, and is used for the blade passage. The O-type grid embedded in the tip clearance consists of 182X13X13 grids. Grid spacing for the first grid point from the blade surface gives $y^+ < 5.0$. The whole grid system has about 1,181,000 grid points. The average number of iterations and CPU time for the converged solution are approximately 3,000 and 3.5 hours with supercomputer of NEC SX-6 (144 GFLOPS), respectively.

Mach numbers in each direction, total pressure and total temperature are given at the inlet. At exit, the hub static pressure ratio has been specified and the radial equilibrium equation is solved along the blade span. A periodic tip clearance model is used to resolve the tip clearance flow explicitly. No-slip and adiabatic wall conditions are used at the wall boundaries. For reducing the computational load, flow field in a single blade passage is simulated by applying periodic boundary condition in the tangential direction.

4. Results and Discussion

4.1. Optimization of blade shape by three different surrogate models

The spanwise distributions of an adiabatic efficiency obtained by numerical simulation are compared with the experimental results at the design flow rate in Fig. 7. In the figure, the thin solid line represents the value determined by numerical simulation, and open rectangular symbols are experimental results. The adiabatic efficiency is obtained by averaging the local values tangentially. It is noted that the adiabatic efficiency obtained by numerical simulation matches relatively well with the experimental results for the

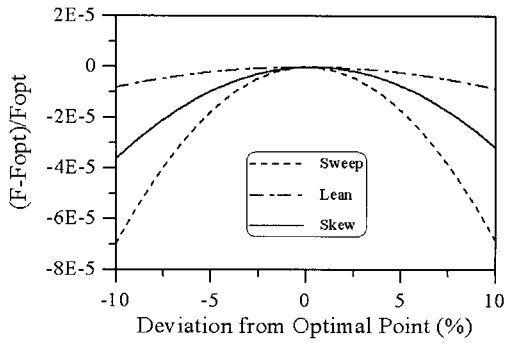

Fig. 8 Sensitivity analysis for optimum shape by RSM

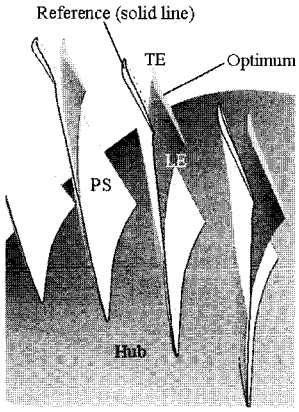

Fig. 9 Optimum blade shape

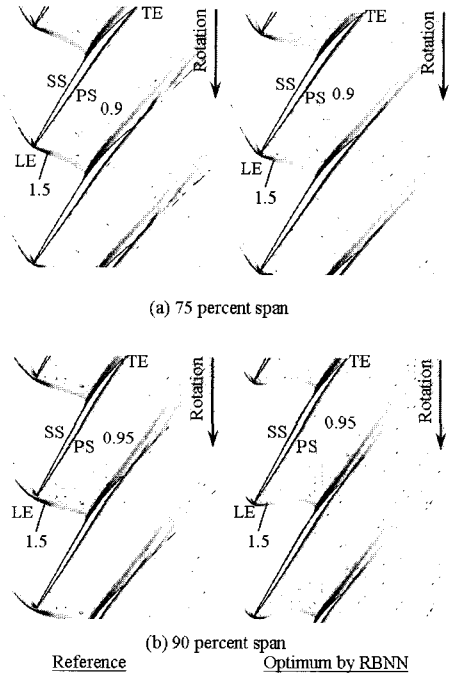

Fig. 10 Mach number contours (interval between contours = 0.05)

reference blade although the adiabatic efficiency is locally overestimated as compared with the experimental one.

The optimization results for the three different surrogate models are summarized in Table 3. The optimum values of the blade sweep and the blade skew are almost same for three surrogate models.

For the RSM, 25 training points determined by a D-optimal design are analyzed. To measure uncertainty in the set of coefficients in a polynominal, ANOVA and regression analysis provided by t-statistic are used[17]. In the present calculation, the value of adjusted R^2 is 0.9378.

The other surrogate models are constructed using the same data set. For KRG the initial parameters for gauss correlation are set properly. SC and EG for RBNN are set by some experiments to generate the reasonable number of neurons. Optimal points are found by sequential quadratic programming (SQP)[14] from all the constructed surrogates.

Predicted and calculated values of adiabatic efficiency at the optimal condition of design variables are shown in Table 4. The predicted efficiencies are obtained by the surrogate models directly. The calculated efficiency is determined through the numerical simulation using the optimum value of design variables. The predicted and calculated efficiency is almost same for the three surrogate models although the band of optimum skew value is wide as shown in Table 3. The prediction error normalized the difference between the predicted and calculated efficient by the predicted efficiency has the lowest value for the RBNN. It should be noted that the optimum results of KRG and RSM are also similar to that of RBNN. Through the shape optimization using three surrogate models, the increase of adiabatic efficiency to the reference is 1.43 percent for RBNN.

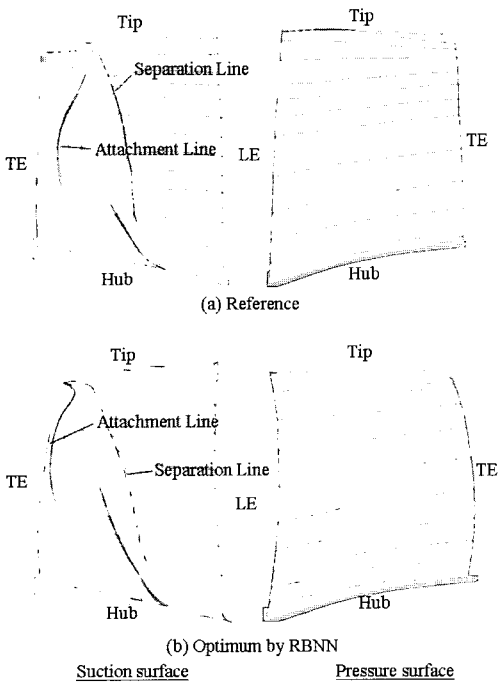

Fig. 11 Limiting streamlines on the blade surfaces

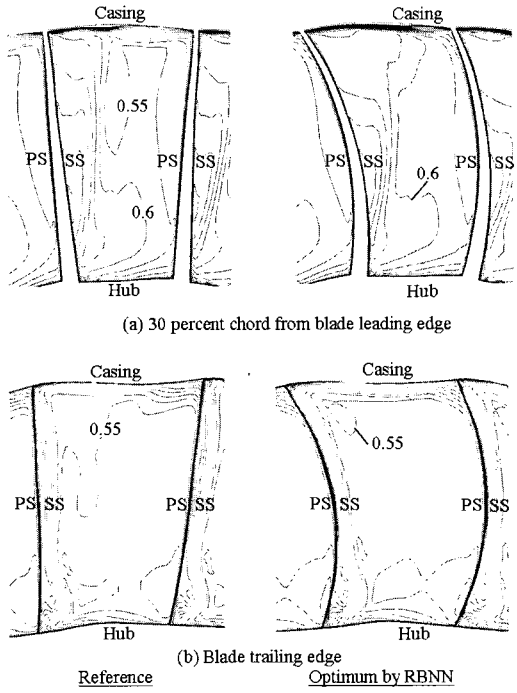

Fig. 12 Axial velocity normalized by sound velocity (interval between contours = 0.05)

Sensitivity analysis for the three design variablesis performed to evaluate the parameter effect on the object function, adiabatic efficiency. The optimal efficiency is Fopt and deviating variable values by 10% from optimal point and objective function values (F) are calculated by polynomial equation generated for RSM.

Figure 8 shows the results of sensitivity analysis for the optimum shape. As shown in the figure, the blade sweep is the most sensitive on the object function. This means that the shape optimization using blade sweep is the most effective to increase an adiabatic efficiency in axial compressor.

Figure 9 shows the three-dimensional blade shapes of the reference and the optimum rotor blades. The blade swept to backward and skewed to the blade pressure side is more effective to increase the adiabatic efficiency in the axial compressor.

4.2 Optimization of blade shape by three different surrogate models

Flow characteristics inside the blade passage for the reference and optimum blades using the results of RBNN are analyzed in the following text.

The spanwise distributions of an adiabatic efficiency for the reference and optimum blades using three surrogate models are compared at the design flow rate as shown in Fig. 7. In the figure, spanwise distribution of adiabatic efficiency has almost same value for three surrogate models. Relatively large increase of adiabatic efficiency is distributed between 50 and 90 percent span. The largest increase in efficiency compared to the reference blade is observed near 75 percent span.

Figure 10, which is perspective view from the casing, shows Mach number contours on the plane of 75 and 90 percent span of the reference and optimum blades. The 75 percent span is the position where relatively large increase in adiabatic efficiency is observed as shown in Fig. 7. In Fig. 10, the inflow is accelerated to supersonic state near the inlet of the blade passage. That is, a bow shock is generated

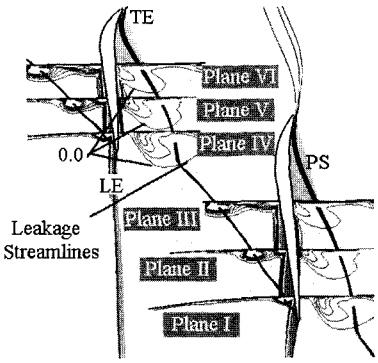

(a) Reference

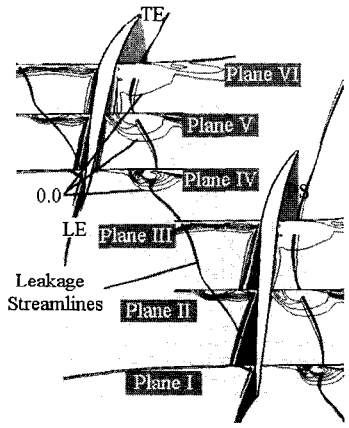

(b) Optimum by RBNN

Fig. 13 Distribution of vorticity on the quasi-orthogonal planes to the leakage vortex and leakage streamlines (interval between contours= 1.0)

upstream of the leading edge of the rotor, and a passage shock develops at the rotor suction surface. It is found that the interference position of the passage shock at the blade suction surface is moved to downstream for the optimum blade as compared to that for the reference one. This means that the local increase of an adiabatic efficiency in spanwise direction, especially at 75 and 90 percent span, has close relation to the position of the passage shock. It is also found that the intensity of high Mach number at the upstream of the blade leading edge and at the blade passage is weakened in case of optimum blade using the results of RBNN.

Figure 11 shows the limiting streamlines on the blade suction and pressure surfaces for the reference and the optimum blades obtained by RBNN. On the blade pressure surface, all limiting streamlines develop from blade leading edge to trailing edge without separation for both cases. On the other hand, separation line is formed on the blade suction surface due to interference between the passage shock and the suction surface boundary layer.

An attachment line is also observed behind the separation line for the reference and optimized cases. Outward radial flow caused by centrifugal effect is also visible at downstream of the separation line. Although the separation line is noticed for both cases, the line for the optimized blades is largely moved towards downstream near the 75 percent span as compared to that for the reference one. Relatively high increase in efficiency shown in Fig. 7 is due to the reduction of separation area on blade surface.

Figure 12, which is the perspective view from downstream, shows the distributions of axial velocity normalized by Mach number at the 30 percent chord from blade leading edge and at the blade trailing edge. As shown in Fig. 12(a), relatively low axial velocity region observed near the blade suction side of the casing for the reference blade is recovered by optimizing the blade stacking line. Uniform axial velocity is also observed at the blade trailing edge for optimum blade.

Figure 13 shows the distributions of the vorticity on six planes nearly perpendicular to the tip leakage vortex and leakage streamlines surrounding the vortex core. In the figure, the vorticity is shown only from zero to seven. The leakage vortex formed on the blade suction surface by the induced velocity generated between a leakage jet flow and a main through flow is shown in the blade passage. For both cases, the leakage vortex is tightly rolled up at upstream of the bow shock with the high vorticity. The vorticity, shown upstream of the bow shock, concentrates on the leakage vortex core. However, the distribution of vorticity expands widely just downstream of the bow shock due to the interference between the leakage vortex and shock wave. As

shown on the plane IV, the region having a vorticity above zero is spread out to about 10 percent of span from the rotor tip of the reference blade. It is found that relatively small region having a vorticity above zero is formed on the plane IV as compared to the reference blade. This is mainly caused by weakened Mach number as shown in Fig. 10. It is noted that the reduced vertical flow in the optimum blade results in uniform axial velocity as shown in Fig. 12.

From the above figures, the increase of adiabatic efficiency for the optimum blade is caused by reduction of the bow shock upstream of blade leading edge. The reduced Mach number induces concentrated vorticity at downstream of the bow shock, thus, makes a uniform axial velocity as compared to reference blade.

5. Conclusion

The shape optimization of rotor blade in a transonic axial compressor rotor is performed by three surrogate models and the three-dimensional Navier-Stokes analysis. By optimizing blade sweep, lean and skew of the rotor, the adiabatic efficiency is increased by 1.43 percent as compared to that of the reference blade at the design flow condition. The shape optimization of rotor blade to enhance an adiabatic efficiency is very effective and reliable for three surrogate models; Kriging, radial basis neural network and response surface methods. Among the design variables of stacking line, blade sweep is the most effective in increase the performance of the compressor rotor. It is found that the increase of adiabatic efficiency for the optimum blade is caused by reduction of the bow shock upstream of blade leading edge and reduction of separation area on blade surface.

References

(1) Watanabe, H. and Zangeneh, M., 2003, "Design of the Blade Geometry of Swept Transonic Fans by 3D Inverse Design," ASME Turbo Expo, GT-2003-38770.

(2) Denton, J. D. and Xu, L., 2002, "The Effects of Lean and Sweep on Transonic Fan Performance," ASME Turbo Expo, GT-2002-30327.

(3) Fischer, A., Riess, W., and Seume, J., 2003, "Performance of Strongly Bowed Stators in a 4-Stage High Speed Compressor," ASME Turbo Expo, GT-2003-38392.

(4) Jang, C.-M., Li, P., and Kim, K.-Y., 2005, "Optimization of Blade Sweep in A Transonic Axial Compressor Rotor," JSME Inter. J. (B), Vol. 48, No. 4, pp. 793~801.

(5) Jang, C.-M., Samad, A., and Kim, K.-Y., 2006, "Optimal Design of Swept, Leaned and Skewed Blades in a Transonic Axial Compressor," ASME Turbo Expo, GT-2006-90384.

(6) Queipo, N.V., Haftka, R.T., Shyy, W., Goel, T., Vaidyanathan, R., and Tucker, P.K., 2005, "Surrogate-Based Analysis and Optimization, Progress in Aerospace Sciences," Vol. 41, pp. 1~28.

(7) Shyy, W., Papila, N., Vaidyanathan, R., and Tucker, K., 2001, "Global Design Optimization for Aerodynamics and Rocket Propulsion Components," Progress in Aerospace Science, Vol. 37, pp. 59~118.

(8) Samad, A., Kim, K.-Y., Goel, T., Haftka, R., and Shyy, W., 2006, "Shape Optimization of Turbomachinery Blade Using Multiple Surrogate Models," ASME FEDSM-2006-98368.

(9) Reid, L. and Moore, R. D., 1978, "Design and Overall Performance of Four Highly-Loaded, High-Speed Inlet Stages for an Advanced, High-Pressure-Ratio Core Compressor." NASA TP-1337.

(10) Myers, R. H. and Montgomery, D. C., 1995, "Response Surface Methodology: Process and Product Optimization Using Designed Experiments," John Wiley & Sons.

(11) Box, M. J. and Draper, N. R., 1971, "Fractional Designs, the XTX Criterion, and Some Related Matters," Technometrics, Vol. 13, No. 4, pp. 731~742.

(12) Martin, J.D. and Simpson, T.W., 2005, "Use of Kriging Models to Approximate Deterministic Computer Models," AIAA Journal, Vol. 43, No. 4, pp. 853~863.

(13) Orr, M.J.L., 1996, "Introduction to Radial Basis Neural Networks, Center for cognitive science," Edinburgh University, Scotland, UK. http://anc.ed.ac.uk/RBNN/.

(14) MATLAB®, The language of technical computing, Release 14. The MathWorks Inc.

(15) Jameson, A., Schmidt, W., andTurkel, E., 1981, "Numerical Solutions of the Euler Equation by Finite Volume Methods Using Runge-Kutta Time Stepping Schemes," AIAA Paper No. 81~1259.

(16) Baldwin, B. S. and Lomax, H., 1978, "Thin Layer Approximation and Algebraic Model for Separated Turbulent Flow," AIAA Paper No. 78~257.

(17) Guinta, A. A., 1997, "Aircraft Multidisciplinary Design Optimization Using Design of Experimental Theory and Response Surface Modeling Methods," Ph. D. Dissertant, Department of Aerospace Engineering, Virginia Polytechnic Institute and State University, Blacksburg, VA.